Article:
Burt, D, Zhang, L, Jung, Y et al. (8 more authors) (2023) Tensile strained direct bandgap GeSn microbridges enabled in GeSn-on-insulator substrates with residual tensile strain. Optics Letters, 48 (3). pp. 735-738. ISSN 0146-9592

https://doi.org/10.1364/ol.476517

Tensile strained direct bandgap GeSn microbridges enabled in GeSn-on-insulator substrates with residual tensile strain

DANIEL BURT,[1,3] LIN ZHANG,[1,3] YONGDUCK JUNG,[1,3] HYO-JUN JOO,[1] YOUNGMIN KIM,[1] MELVINA CHEN,[1] BONGKWON SON,[1] WEIJUN FAN,[1] ZORAN IKONIC,[2] CHUAN SENG TAN,[2] DONGUK NAM[1,*]

[1]*School of Electrical and Electronic Engineering, Nanyang Technological University, 50 Nanyang Avenue, Singapore 639798, Singapore*
[2] *School of Electronic and Electrical Engineering, University of Leeds, Leeds LS2 9JT, UK*
[3] *The authors contributed equally to this work.*
**Corresponding author: dnam@ntu.edu.sg*

Received XX Month XXXX; revised XX Month, XXXX; accepted XX Month XXXX; posted XX Month XXXX (Doc. ID XXXXX); published XX Month XXXX

Despite having achieved drastically improved lasing characteristics by harnessing tensile strain, the current methods of introducing a sizeable tensile strain into GeSn lasers require complex fabrication processes, thus reducing the viability of the lasers for practical applications. The geometric strain amplification is a simple technique that can concentrate residual and small tensile strain into localized and large tensile strain. However, the technique is not suitable for GeSn due to the intrinsic compressive strain introduced during the conventional epitaxial growth. In this paper, we demonstrate the geometrical strain amplification in GeSn by employing a tensile strained GeSn-on-insulator (GeSnOI) substrate. This work offers exciting opportunities in developing practical wavelength-tunable lasers for realizing fully integrated photonic circuits.

Silicon (Si) photonics has the potential to enable a wide range of exciting applications, including optical data communications and sensor technologies.[1] Currently, Si photonics relies on III-V heterogeneous integration to provide an on-chip laser.[2] Despite remarkable progress with this hybrid integration approach, III-V materials are fundamentally incompatible with the industry-standard complementary metal-oxide-semiconductor (CMOS) technology. Germanium (Ge) has been extensively explored as a suitable candidate for developing on-chip lasers[3–5] owing to its CMOS compatibility and near-direct bandgap configuration (~140 meV offset between the direct Γ- and indirect L-conduction valleys).

By introducing a considerable mechanical tensile strain, the energy difference between the direct Γ- and indirect L-valleys can be reduced, and with enough strain, Ge can become a direct bandgap material, thus drastically improving light emission.[6–16] Low-threshold lasing at cryogenic temperatures has been demonstrated in Ge under both large uniaxial[11,12] and biaxial[13] tensile strains. An even larger tensile strain is required to improve the directness towards room-temperature operation.[17] However, it is practically challenging to introduce such a large tensile strain into a suitable lasing geometry.

Alloying Ge with tin (Sn) to form the binary alloy GeSn is another promising approach to achieve a CMOS compatible light source.[18–24] An optically pumped laser was demonstrated at cryogenic temperatures in a direct bandgap $Ge_{0.875}Sn_{0.125}$ waveguide[18], which motivated many researchers to further increase the Sn content in order to achieve higher operating temperatures.[19,20,25] By increasing the Sn content to 20 at%, an operating temperature of 270 K[25] was achieved. Recently, room-temperature operation has also been reported.[26,27] Furthermore, electrically-injected GeSn lasers operating at cryogenic temperatures[28] and light-emitting diodes (LEDs) operating at room temperature[29] have also recently been demonstrated, highlighting the great potential of this approach.

Recently, a hybrid approach combining low Sn content GeSn alloys with tensile strain engineering has been theoretically proposed.[30,31] This approach offers the advantage of a large directness at a much lower tensile strain compared to Ge and much a lower Sn content compared to high Sn content GeSn alloys. An ultra-low threshold of 0.8 kW cm^{-2} was achieved from a $Ge_{0.95}Sn_{0.05}$ alloy under 1.4% biaxial tensile strain[32], as well as the first demonstration of continuous-wave lasing in GeSn alloys. Lasing from GeSn with a higher Sn content of 16 at% under a uniaxial tensile strain has also been demonstrated[33], exhibiting a threshold power density of 10 kW cm^{-2} and almost room temperature operation of 273 K. The two reports of tensile strained GeSn lasers used external stressors such as silicon nitride (Si_3N_4) thin films[32] and Ge buffer layers[33] to induce a large tensile strain that can overcome the residual compressive strain in GeSn. However, the fabrication processes to employ external stressors are exceedingly complicated, thus limiting the compatibility to CMOS processes.

The geometric strain amplification technique is a straightforward method that has been widely used to concentrate residual and small tensile strain in a layer into localized and large tensile strain in a properly designed structure[6,11,34]. Using this technique, several researchers have demonstrated excellent lasing characteristics in strained Ge[11,12]. Unfortunately, this powerful technique cannot be used for GeSn because epitaxially grown GeSn layers obtain intrinsic compressive strain during the growth process. The geometric strain

amplification technique will result in a detrimental amplified compressive strain in GeSn, not the desired tensile strain. Therefore, to exploit such a powerful technique for developing tensile strained GeSn lasers, it is crucial to invent a method to obtain an isolated tensile strained GeSn layer.

In this paper, we demonstrate the application of the geometrical strain amplification technique to GeSn by utilizing a low Sn content tensile strained GeSn-on-insulator (GeSnOI) substrate. Raman spectroscopy confirmed that uniaxial tensile strain of up to 1.23% can be induced in microbridge structures, which results in an order-of-magnitude enhanced direct bandgap light emission in strained GeSn compared to unstrained GeSn. The emission wavelength in unstrained GeSn was ~1900 nm, which was redshifted by ~500 nm upon the introduction of 1.23% uniaxial strain. Temperature-dependent PL studies combined with theoretical calculations using the **k •p** method uncovered a cross-over from an indirect to a direct bandgap material for GeSn microbridges with sizeable uniaxial tensile strains. Our results offer a step forward to efficient wavelength-tunable tensile strained GeSn lasers towards CMOS compatible optoelectronics.

To obtain an amplified uniaxial tensile strain in the GeSn microbridges using the geometric strain amplification technique, the intrinsic stress in the GeSn layer must be tensile. However, GeSn layers grown on Ge buffer layers, which is a convention to grow high-quality GeSn layers, possess compressive residual strain due to the larger lattice constant of GeSn compared to Ge. To obtain a tensile strained GeSn layer, a lower Sn content GeSn layer of 6.0 at% was grown on top of a higher Sn content GeSn layer of ~10 at%.[35]

A direct bonding technique was utilized to transfer the GeSn layers onto dual insulators and form GeSnOI.[23] Figure 1 (a) shows the transmission electron microscopy (TEM) cross-sectional image of the tensile GeSnOI substrate used in this study. It should be noted that the highly defective interface between the GeSn and Ge buffer layers in the as-grown substrate was removed during the bonding process, improving the overall quality of the material.[36] The final material stack consists of a ~100 nm tensile strained $Ge_{0.94}Sn_{0.06}$ layer on top of dual insulators (Al_2O_3/SiO_2) on a Si substrate (not shown).

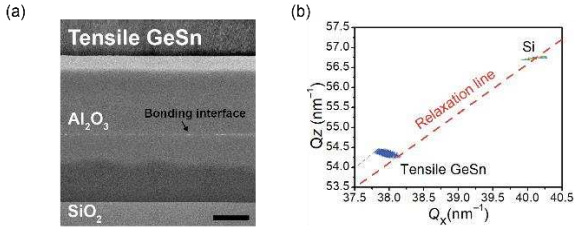

FIG. 1. (a) Cross-sectional TEM image of the tensile strained GeSnOI substrate. Scale bar, 100 nm. (b) RSM map of the tensile strained GeSnOI substrate with the relaxation line indicated in red.

High-resolution X-ray diffraction (HR-XRD) was used to determine the magnitude of the residual tensile strain as well as the Sn content in the GeSnOI layer. The reciprocal space map (RSM) around the (224) order of the GeSnOI layer is shown in Fig. 1(b). The normalized tilted angle of the GeSnOI layer (after the bonding process) is based on the GeSn peak in the RSM (004) image. The Sn content of the GeSnOI layer was determined to be 6.0 at% and calculated by considering the deviation from the theoretical values of the Sn and Ge lattice constants considering Vegard's law. We extracted the intrinsic tensile strain of the GeSnOI layer to be ~0.3%. The methodology to calculate the intrinsic strain and the Sn content were taken from [37].

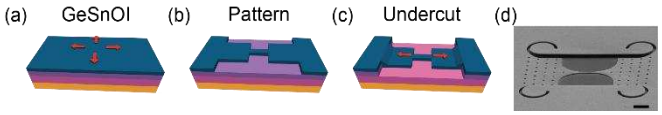

FIG. 2. (a-c) Schematic representation of the microbridge fabrication process. (d) Tilted view SEM image of a fabricated microbridge. Scale bar, 5 μm.

Microbridges were fabricated on the tensile GeSnOI substrate according to the schematic in Fig. 2(a-c). Figure 2(d) shows a scanning electron microscopy (SEM) image of a fabricated microbridge which has been brought into contact with the underlying substrate. In-depth details of the material growth, bonding and device fabrication are provided in the supplementary information.

To verify and quantify the uniaxial tensile strain in the microbridges. Figure 3(a) shows the measured Raman spectra of a relaxed (i.e., 0% strain) and two strained bridges with pad lengths of 50 μm and 75 μm, respectively. The 0% strain measurements were conducted on broken bridges where the strain has fully relaxed due to fracture. The bulk GeSnOI substrate was also measured as a reference. The bridge width and height were fixed for all bridges as 1 μm and 7.5 μm, respectively, and therefore, the amount of strain should be dependent only on the pad length. We observed distinct peak shifts of 2.25 cm^{-1} and 3.30 cm^{-1} for the two devices with 50 μm and 75 μm, respectively. Using a Raman-strain coefficient[38] of 269 cm^{-1}, the uniaxial tensile strain values were calculated as 0.83% and 1.23%, respectively. Higher tensile strain can be induced by further increasing the pad size, as proven in the previous demonstration of strain amplification in Ge[9] and Si[34].

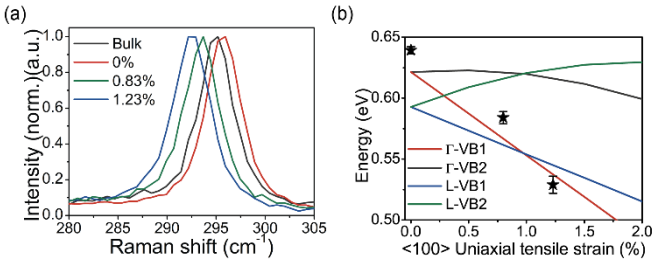

FIG. 3. (a) Raman spectra of relaxed and strained GeSn microbridges. (b) Calculated bandgap energies as a function of uniaxial tensile strain. The experimental values of the Γ-VB1 bandgap energies are shown as stars.

Figure 3(b) shows the calculated bandgap energies as a function of uniaxial tensile strain along the <100> direction with the experimentally extracted values of the Γ-VB1 band gap energies shown as black stars. The experimental values of the Γ-VB1 bandgap energy were extracted using a Gaussian fit from the low-temperature PL measurements presented in Fig. 4(a). Calculations were conducted using the 8-band k·p method to determine the effect of the uniaxial tensile strain on the bandgap energies of the microbridges at a temperature of 4 K. The parameters used in the calculation were taken from ref.[39] In the relaxed state, the GeSn bridge with the Sn content of 6.0 at% is an indirect bandgap material. The calculations predict that a cross-over to a direct bandgap material occurs at a uniaxial tensile strain value of ~0.95%. Therefore, we can infer from these calculations that we have experimentally induced sufficient tensile strain to convert the microbridge into a direct bandgap configuration. There is a discrepancy between the theoretically predicted and experimentally extracted values of Γ-VB1. We note that there can be several potential reasons for such a discrepancy that include the choice of parameters used in the **k•p** calculations, small uncertainties in extracting the Sn content from XRD and non-linear effects at higher strain values not accounted for with our linear Raman strain-shift coefficient.

Photoluminescence (PL) studies were conducted to study the effect of the uniaxial tensile strain on the optical emission of the microbridges. Figures 4(a) and (b) shows the PL spectra of the 0%, 0.83%, and 1.23% strained microbridges at 4 K and 125 K, respectively, for a fixed pump power of 3 mW. The bridges were optically pumped with a pulsed laser. The pump wavelength was 1550-nm, with a repetition rate of 1MHz, and a pulse width of 5 ns. The emission spectrum features beyond 2300 nm for the 1.23% strained GeSn such as a dip at ~2300 nm is due to FTIR artifacts and water absorption lines. Despite these distortions, the emission peak position is shifted by more than 400 nm when GeSn is strained up to 1.23%, which qualitatively agrees with the theoretically calculated Γ-VB1 band gap energies as a function of strain (Fig. 3(b)). We observed a small redshift (~10 nm) in the peak positions as the temperature increased from 4K to 125K due to bandgap narrowing. It should also be noted that, the strain in the bridge cannot change with temperature as the bridge is stuck to the underlying layer and not free to move with the thermal expansion changes. Furthermore, the integrated intensity increases by approximately an order of magnitude with the introduction of uniaxial tensile strain. This enhanced light emission is a result of the improved directness (i.e., a reduced energy offset between the Γ- and L-valleys), which has been previously reported in Ge microbridges under uniaxial tensile strain[9] and GeSn alloys with increasing Sn content[18,40]. As the directness increases with the introduction of uniaxial tensile strain, a more significant fraction of photoexcited carriers occupies the direct Γ-valley, where they can contribute to direct spontaneous emission.

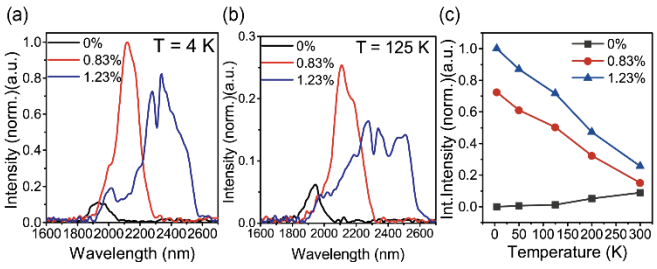

FIG. 4. Emission spectra of relaxed and strained GeSn microbridges at (a) 4 K and (b) 125 K. (c) Normalized integrated emission intensity of the GeSn microbridges as a function of temperature.

Figure 4(c) presents the temperature dependence of the integrated PL intensity (i.e., the integrated area for each spectrum) for the relaxed and strained microbridges. In the case of the relaxed microbridge, a rapid decrease in the integrated intensity of the direct emission is observed as the temperature is decreased from 300 K to 4 K. This behavior is typical for indirect bandgap materials such as relaxed Ge as the direct Γ-valley is not the conduction band minima, resulting in a significantly lowered electron population in the Γ-valley at lower temperatures[4]. At higher temperatures, the electrons in the L-valley are thermally activated and can populate the Γ-valley where they can contribute to direct spontaneous emission. In contrast, for both the microbridges under tensile strain, the integrated intensity strongly increases as the temperature is decreased to 4 K. Traditional direct bandgap materials (e.g., III-V materials) also exhibit a steadily increasing PL intensity with decreasing temperatures,[41] which is attributed to an exponential decrease in non-radiative electron-hole recombination processes. In the case of tensile strained GeSn attaining direct bandgap but with a low directness, the increase of direct spontaneous emission at lower temperatures can be mainly accredited to the increased electron population in the Γ-valley that is the conduction band minimum.[42] Therefore, the significantly increased emission intensity at lower temperatures provides strong evidence of a transition into a direct bandgap material for the GeSn microbridges under uniaxial tensile strain. It should be noted that the k·p calculations predict that the microbridge under 0.83% should still be an indirect bandgap material (Fig. 3(b)), which is contradictory to the experimental results (Fig. 4(c)). This discrepancy can be attributed to uncertainties in experimental conditions (e.g., determining the Sn content) and theoretical calculations (e.g., choice of parameters used). It should be noted that the method used to calculate the integrated intensity for each spectrum did not account for the artifacts present in the spectrum. While this may cause some small errors, there is a very clear temperature-dependent trend of the PL at different strains, which we repeatedly observed for many devices. We would like to note that this increasing PL trend at lower temperatures for the 1.23%-strained devices remains valid even when the spectra are slightly distorted because the atmospheric absorption will influence the integrated PL intensity at different temperatures at the same ratio. The goal of this study was to present a methodology for creating a tensile strained GeSnOI substrate that can be utilized with the geometric strain amplification method. This platform will also be ideal for a comprehensive study of the influence of tensile strain on the bandstructure of GeSn alloys by using advanced analytical methods[25] which will be addressed in future works.

For simplicity, in this study, we chose a thin active layer (~100 nm) below the critical thickness of relaxation (which we calculated to be ~180 nm). It should be noted that for the extended mid-infrared applications, it is possible to increase the thickness of the active layer substantially. The maximum thickness of the active layer is determined by the lattice mismatch between the two topmost GeSn layers during the growth. For example, in this study, we targeted to achieve Sn contents of 6% and 10% for the topmost and the second-to-the-topmost layers. In this case, the difference in the Sn content is 4%. Lowering this difference in the Sn content will allow growing a thicker active layer. Even though the tensile strain in the active layer can be reduced in this case, our geometrical strain amplification method can amplify the initial strain as long as the initial strain is tensile.

In summary, we have presented a method of achieving sizeable uniaxial tensile strain in low Sn content GeSn alloys by harnessing the geometric strain amplification technique. The use of a tensile strained GeSnOI substrate allowed the utilization of the simple strain amplification technique, enabling the introduction of uniaxial tensile strain of up to 1.23%. Raman spectroscopy was used to confirm a level of uniaxial tensile strain. Bandstructure calculations with the **k•p** method combined with PL measurements revealed that the achieved tensile strain was sufficient to convert the 6.0 at% GeSnOI layer into a direct bandgap material. We also confirmed that the strain, and therefore, the emission wavelength can be tuned by a simple lithographic design by changing the pad length. Our work provides opportunities to realize efficient wavelength-tunable strained GeSn lasers.

DATA AVALIABILITY

The data that support the findings of this study are available from the corresponding author upon reasonable request.

DISCLOSURES

The authors declare no conflicts of interest.

ACKNOWLEDGMENTS

The research of the project was in part supported by Ministry of Education, Singapore, under grant AcRF TIER 1 (RG 115/21). The

research of the project was also supported by Ministry of Education, Singapore, under grant AcRF TIER 2 (MOE2018-T2-2-011 (S)). This work is also supported by National Research Foundation of Singapore through the Competitive Research Program (NRF-CRP19-2017-01). This work is also supported by National Research Foundation of Singapore through the NRF-ANR Joint Grant (NRF2018-NRF-ANR009 TIGER). This work is also supported by the iGrant of Singapore A*STAR AME IRG (A2083c0053). The authors would like to acknowledge and thank the Nanyang NanoFabrication Centre (N2FC).

Supplemental document

See Supplement for supporting content.

References

1. R. Jones, H. Rong, H.-F. Liu, and M. Paniccia, in *Silicon Photonics* (John Wiley & Sons, Ltd, 2008), pp. 297–325.
2. S. Chen, W. Li, J. Wu, Q. Jiang, M. Tang, S. Shutts, S. N. Elliott, A. Sobiesierski, A. J. Seeds, I. Ross, P. M. Smowton, and H. Liu, Nat. Photonics **10**, 307 (2016).
3. Z. Qi, H. Sun, M. Luo, Y. Jung, and D. Nam, J. Phys. Condens. Matter **30**, 334004 (2018).
4. X. Sun, J. Liu, L. C. Kimerling, and J. Michel, Appl. Phys. Lett. **95**, 011911 (2009).
5. J. Liu, X. Sun, R. Camacho-Aguilera, L. C. Kimerling, and J. Michel, Opt. Lett. **35**, 679 (2010).
6. D. Nam, D. S. Sukhdeo, J. H. Kang, J. Petykiewicz, J. H. Lee, W. S. Jung, J. Vučković, M. L. Brongersma, and K. C. Saraswat, Nano Lett. **13**, 3118 (2013).
7. J. Petykiewicz, D. Nam, D. S. Sukhdeo, S. Gupta, S. Buckley, A. Y. Piggott, J. Vučković, and K. C. Saraswat, Nano Lett. **16**, 2168 (2016).
8. D. Nam, D. Sukhdeo, S.-L. Cheng, A. Roy, K. Chih-Yao Huang, M. Brongersma, Y. Nishi, and K. Saraswat, Appl. Phys. Lett. **100**, 131112 (2012).
9. M. J. Süess, R. Geiger, R. A. Minamisawa, G. Schiefler, J. Frigerio, D. Chrastina, G. Isella, R. Spolenak, J. Faist, and H. Sigg, Nat. Photonics **7**, 466 (2013).
10. Y. Jung, Y. Kim, D. Burt, H.-J. Joo, D.-H. Kang, M. Luo, M. Chen, L. Zhang, C. S. Tan, and D. Nam, Opt. Express **29**, 14174 (2021).
11. F. T. Armand Pilon, A. Lyasota, Y.-M. Niquet, V. Reboud, V. Calvo, N. Pauc, J. Widiez, C. Bonzon, J. M. Hartmann, A. Chelnokov, J. Faist, and H. Sigg, Nat. Commun. **10**, 2724 (2019).
12. S. Bao, D. Kim, C. Onwukaeme, S. Gupta, K. Saraswat, K. H. Lee, Y. Kim, D. Min, Y. Jung, H. Qiu, H. Wang, E. A. Fitzgerald, C. S. Tan, and D. Nam, Nat. Commun. **8**, 1845 (2017).
13. A. Elbaz, M. El Kurdi, A. Aassime, S. Sauvage, X. Checoury, I. Sagnes, C. Baudot, F. Boeuf, and P. Boucaud, APL Photonics **3**, 106102 (2018).
14. D. Nam, D. Sukhdeo, A. Roy, K. Balram, S.-L. Cheng, K. C.-Y. Huang, Z. Yuan, M. Brongersma, Y. Nishi, D. Miller, and K. Saraswat, Opt. Express **19**, 25866 (2011).
15. D. S. Sukhdeo, D. Nam, J.-H. Kang, M. L. Brongersma, and K. C. Saraswat, Photonics Res. **2**, A8 (2014).
16. D. Nam, D. S. Sukhdeo, S. Gupta, J.-H. Kang, M. L. Brongersma, and K. C. Saraswat, IEEE J. Sel. Top. Quantum Electron. **20**, 16 (2014).
17. S. Gupta, D. Nam, J. Vuckovic, and K. Saraswat, Phys. Rev. B **97**, 155127 (2018).
18. S. Wirths, R. Geiger, N. von den Driesch, G. Mussler, T. Stoica, S. Mantl, Z. Ikonic, M. Luysberg, S. Chiussi, J. M. Hartmann, H. Sigg, J. Faist, D. Buca, and D. Grützmacher, Nat. Photonics **9**, 88 (2015).
19. V. Reboud, A. Gassenq, N. Pauc, J. Aubin, L. Milord, Q. M. Thai, M. Bertrand, K. Guilloy, D. Rouchon, J. Rothman, T. Zabel, F. Armand Pilon, H. Sigg, A. Chelnokov, J. M. Hartmann, and V. Calvo, Appl. Phys. Lett. **111**, 92101 (2017).
20. Q. M. Thai, N. Pauc, J. Aubin, M. Bertrand, J. Chrétien, V. Delaye, A. Chelnokov, J.-M. Hartmann, V. Reboud, and V. Calvo, Opt. Express **26**, 32500 (2018).
21. D. Stange, S. Wirths, R. Geiger, C. Schulte-Braucks, B. Marzban, N. von den Driesch, G. Mussler, T. Zabel, T. Stoica, J.-M. Hartmann, S. Mantl, Z. Ikonic, D. Grützmacher, H. Sigg, J. Witzens, and D. Buca, ACS Photonics **3**, 1279 (2016).
22. H.-J. Joo, Y. Kim, D. Burt, Y. Jung, L. Zhang, M. Chen, S. J. Parluhutan, D.-H. Kang, C. Lee, S. Assali, Z. Ikonic, O. Moutanabbir, Y.-H. Cho, C. S. Tan, and D. Nam, Appl. Phys. Lett. **119**, 201101 (2021).
23. D. Burt, H.-J. Joo, Y. Jung, Y. Kim, M. Chen, Y.-C. Huang, and D. Nam, Opt. Express **29**, 28959 (2021).
24. Y. Kim, S. Assali, D. Burt, Y. Jung, H.-J. Joo, M. Chen, Z. Ikonic, O. Moutanabbir, and D. Nam, Adv. Opt. Mater. **n/a**, 2101213 (2021).
25. Y. Zhou, W. Dou, W. Du, S. Ojo, H. Tran, S. A. Ghetmiri, J. Liu, G. Sun, R. Soref, J. Margetis, J. Tolle, B. Li, Z. Chen, M. Mortazavi, and S. Q. Yu, ACS Photonics **6**, 1434 (2019).
26. J. Chrétien, Q. M. Thai, M. Frauenrath, L. Casiez, A. Chelnokov, V. Reboud, J. M. Hartmann, M. El Kurdi, N. Pauc, and V. Calvo, Appl. Phys. Lett. **120**, 51107 (2022).
27. A. Bjelajac, M. Gromovyi, E. Sakat, B. Wang, G. Patriarche, N. Pauc, V. Calvo, P. Boucaud, F. Boeuf, A. Chelnokov, V. Reboud, M. Frauenrath, J.-M. Hartmann, and M. El Kurdi, Opt. Express **30**, 3954 (2022).
28. Y. Zhou, Y. Miao, S. Ojo, H. Tran, G. Abernathy, J. M. Grant, S. Amoah, G. Salamo, W. Du, J. Liu, J. Margetis, J. Tolle, Y. Zhang, G. Sun, R. A. Soref, B. Li, and S.-Q. Yu, Optica **7**, 924 (2020).
29. M. Oehme, J. Werner, M. Gollhofer, M. Schmid, M. Kaschel, E. Kasper, and J. Schulze, IEEE Photonics Technol. Lett. **23**, 1751 (2011).
30. D. Rainko, Z. Ikonic, A. Elbaz, N. von den Driesch, D. Stange, E. Herth, P. Boucaud, M. El Kurdi, D. Grützmacher, and D. Buca, Sci. Rep. **9**, 259 (2019).
31. S. Gupta, B. Magyari-Köpe, Y. Nishi, and K. C. Saraswat, J. Appl. Phys. **113**, 073707 (2013).
32. A. Elbaz, D. Buca, N. von den Driesch, K. Pantzas, G. Patriarche, N. Zerounian, E. Herth, X. Checoury, S. Sauvage, I. Sagnes, A. Foti, R. Ossikovski, J. M. Hartmann, F. Boeuf, Z. Ikonic, P. Boucaud, D. Grützmacher, and M. El Kurdi, Nat. Photonics **14**, 375 (2020).
33. J. Chrétien, N. Pauc, F. Armand Pilon, M. Bertrand, Q. M. Thai, L. Casiez, N. Bernier, H. Dansas, P. Gergaud, E. Delamadeleine, R. Khazaka, H. Sigg, J. Faist, A. Chelnokov, V. Reboud, J. M. Hartmann, and V. Calvo, ACS Photonics **6**, 2462 (2019).
34. R. A. Minamisawa, M. J. Süess, R. Spolenak, J. Faist, C. David, J. Gobrecht, K. K. Bourdelle, and H. Sigg, Nat. Commun. **3**, 1096 (2012).
35. S. Wirths, Z. Ikonic, A. T. Tiedemann, B. Holländer, T. Stoica, G. Mussler, U. Breuer, J. M. Hartmann, A. Benedetti, S. Chiussi, D. Grützmacher, S. Mantl, and D. Buca, Appl. Phys. Lett. **103**, 192110 (2013).
36. A. Elbaz, R. Arefin, E. Sakat, B. Wang, E. Herth, G. Patriarche, A. Foti, R. Ossikovski, S. Sauvage, X. Checoury, K. Pantzas, I. Sagnes, J. Chrétien, L. Casiez, M. Bertrand, V. Calvo, N. Pauc, A. Chelnokov, P. Boucaud, F. Boeuf, V. Reboud, J. M. Hartmann, and M. El Kurdi, ACS Photonics **7**, 2713 (2020).
37. F. Gencarelli, B. Vincent, J. Demeulemeester, A. Vantomme, A. Moussa, A. Franquet, A. Kumar, H. Bender, J. Meersschaut, W. Vandervorst, R. Loo, M. Caymax, K. Temst, and M. Heyns, ECS J. Solid State Sci. Technol. **2**, P134 (2013).
38. S. An, Y. C. Tai, K. C. Lee, S. H. Shin, H. H. Cheng, G. E. Chang, and M. Kim, Nanotechnology **32**, 355704 (2021).
39. D. Rainko, Z. Ikonic, N. Vukmirović, D. Stange, N. von den Driesch, D. Grützmacher, and D. Buca, Sci. Rep. **8**, 15557 (2018).
40. R. Chen, H. Lin, Y. Huo, C. Hitzman, T. I. Kamins, and J. S. Harris, Appl. Phys. Lett. **99**, 181125 (2011).
41. L. Pavesi and M. Guzzi, J. Appl. Phys. **75**, 4779 (1994).
42. D. Stange, S. Wirths, N. Von Den Driesch, G. Mussler, T. Stoica, Z. Ikonic, J. M. Hartmann, S. Mantl, D. Grützmacher, and D. Buca, ACS Photonics **2**, 1539 (2015).

References for review

1. R. Jones, H. Rong, H.-F. Liu, and M. Paniccia, "Silicon Photonic Applications," in *Silicon Photonics* (John Wiley & Sons, Ltd, 2008), pp. 297–325.
2. S. Chen, W. Li, J. Wu, Q. Jiang, M. Tang, S. Shutts, S. N. Elliott, A. Sobiesierski, A. J. Seeds, I. Ross, P. M. Smowton, and H. Liu, "Electrically pumped continuous-wave III-V quantum dot lasers on silicon," Nat. Photonics **10**(5), 307–311 (2016).
3. Z. Qi, H. Sun, M. Luo, Y. Jung, and D. Nam, "Strained germanium nanowire optoelectronic devices for photonic-integrated circuits," J. Phys. Condens. Matter **30**(33), 334004 (2018).
4. X. Sun, J. Liu, L. C. Kimerling, and J. Michel, "Direct gap photoluminescence of n-type tensile-strained Ge-on-Si," Appl. Phys. Lett. **95**, 011911 (2009).
5. J. Liu, X. Sun, R. Camacho-Aguilera, L. C. Kimerling, and J. Michel, "Ge-on-Si laser operating at room temperature," Opt. Lett. **35**(5), 679 (2010).
6. D. Nam, D. S. Sukhdeo, J. H. Kang, J. Petykiewicz, J. H. Lee, W. S. Jung, J. Vučković, M. L. Brongersma, and K. C. Saraswat, "Strain-induced pseudoheterostructure nanowires confining carriers at room temperature with nanoscale-tunable band profiles," Nano Lett. **13**(7), 3118–3123 (2013).
7. J. Petykiewicz, D. Nam, D. S. Sukhdeo, S. Gupta, S. Buckley, A. Y. Piggott, J. Vučković, and K. C. Saraswat, "Direct Bandgap Light Emission from Strained Germanium Nanowires Coupled with High-Q Nanophotonic Cavities," Nano Lett. **16**(4), 2168–2173 (2016).
8. M. J. Süess, R. Geiger, R. A. Minamisawa, G. Schiefler, J. Frigerio, D. Chrastina, G. Isella, R. Spolenak, J. Faist, and H. Sigg, "Analysis of enhanced light emission from highly strained germanium microbridges," Nat. Photonics **7**(6), 466–472 (2013).
9. Y. Jung, Y. Kim, D. Burt, H.-J. Joo, D.-H. Kang, M. Luo, M. Chen, L. Zhang, C. S. Tan, and D. Nam, "Biaxially strained germanium crossbeam with a high-quality optical cavity for on-chip laser applications," Opt. Express **29**(10), 14174 (2021).
10. F. T. Armand Pilon, A. Lyasota, Y.-M. Niquet, V. Reboud, V. Calvo, N. Pauc, J. Widiez, C. Bonzon, J. M. Hartmann, A. Chelnokov, J. Faist, and H. Sigg, "Lasing in strained germanium microbridges," Nat. Commun. **10**, 2724 (2019).
11. S. Bao, D. Kim, C. Onwukaeme, S. Gupta, K. Saraswat, K. H. Lee, Y. Kim, D. Min, Y. Jung, H. Qiu, H. Wang, E. A. Fitzgerald, C. S. Tan, and D. Nam, "Low-threshold optically pumped lasing in highly strained germanium nanowires," Nat. Commun. **8**, 1845 (2017).
12. A. Elbaz, M. El Kurdi, A. Aassime, S. Sauvage, X. Checoury, I. Sagnes, C. Baudot, F. Boeuf, and P. Boucaud, "Germanium microlasers on metallic pedestals," APL Photonics **3**(10), 106102 (2018).
13. D. Nam, D. Sukhdeo, A. Roy, K. Balram, S.-L. Cheng, K. C.-Y. Huang, Z. Yuan, M. Brongersma, Y. Nishi, D. Miller, and K. Saraswat, "Strained germanium thin film membrane on silicon substrate for optoelectronics," Opt. Express **19**(27), 25866 (2011).
14. D. S. Sukhdeo, D. Nam, J.-H. Kang, M. L. Brongersma, and K. C. Saraswat, "Direct bandgap germanium-on-silicon inferred from 5.7% 〈100〉 uniaxial tensile strain [Invited]," Photonics Res. **2**(3), A8 (2014).
15. D. Nam, D. S. Sukhdeo, S. Gupta, J.-H. Kang, M. L. Brongersma, and K. C. Saraswat, "Study of Carrier Statistics in Uniaxially Strained Ge for a Low-Threshold Ge Laser," IEEE J. Sel. Top. Quantum Electron. **20**(4), 16–22 (2014).
16. D. Nam, D. Sukhdeo, S.-L. Cheng, A. Roy, K. Chih-Yao Huang, M. Brongersma, Y. Nishi, and K. Saraswat, "Electroluminescence from strained germanium membranes and implications for an efficient Si-compatible laser," Appl. Phys. Lett. **100**(13), 131112 (2012).
17. S. Gupta, D. Nam, J. Vuckovic, and K. Saraswat, "Room temperature lasing unraveled by a strong resonance between gain and parasitic absorption in uniaxially strained germanium," Phys. Rev. B **97**(15), 155127 (2018).
18. S. Wirths, R. Geiger, N. von den Driesch, G. Mussler, T. Stoica, S. Mantl, Z. Ikonic, M. Luysberg, S. Chiussi, J. M. Hartmann, H. Sigg, J. Faist, D. Buca, and D. Grützmacher, "Lasing in direct-bandgap GeSn alloy grown on Si," Nat. Photonics **9**(2), 88–92 (2015).
19. V. Reboud, A. Gassenq, N. Pauc, J. Aubin, L. Milord, Q. M. Thai, M. Bertrand, K. Guilloy, D. Rouchon, J. Rothman, T. Zabel, F. Armand Pilon, H. Sigg, A. Chelnokov, J. M. Hartmann, and V. Calvo, "Optically pumped GeSn micro-disks with 16% Sn lasing at 3.1 μm up to 180 K," Appl. Phys. Lett. **111**(9), 92101 (2017).
20. Q. M. Thai, N. Pauc, J. Aubin, M. Bertrand, J. Chrétien, V. Delaye, A. Chelnokov, J.-M. Hartmann, V. Reboud, and V. Calvo, "GeSn heterostructure micro-disk laser operating at 230 K," Opt. Express **26**(25), 32500–32508 (2018).
21. D. Stange, S. Wirths, R. Geiger, C. Schulte-Braucks, B. Marzban, N. von den Driesch, G. Mussler, T. Zabel, T. Stoica, J.-M. Hartmann, S. Mantl, Z. Ikonic, D. Grützmacher, H. Sigg, J. Witzens, and D. Buca, "Optically Pumped GeSn Microdisk Lasers on Si," ACS Photonics **3**(7), 1279–1285 (2016).
22. H.-J. Joo, Y. Kim, D. Burt, Y. Jung, L. Zhang, M. Chen, S. J. Parluhutan, D.-H. Kang, C. Lee, S. Assali, Z. Ikonic, O. Moutanabbir, Y.-H. Cho, C. S. Tan, and D. Nam, "1D photonic crystal direct bandgap GeSn-on-insulator laser," Appl. Phys. Lett. **119**(20), 201101 (2021).
23. D. Burt, H.-J. Joo, Y. Jung, Y. Kim, M. Chen, Y.-C. Huang, and D. Nam, "Strain-relaxed GeSn-on-insulator (GeSnOI) microdisks," Opt. Express **29**(18), 28959–28967 (2021).
24. Y. Kim, S. Assali, D. Burt, Y. Jung, H.-J. Joo, M. Chen, Z. Ikonic, O. Moutanabbir, and D. Nam, "Enhanced GeSn Microdisk Lasers Directly Released on Si," Adv. Opt. Mater. **n/a**(n/a), 2101213 (2021).
25. Y. Zhou, W. Dou, W. Du, S. Ojo, H. Tran, S. A. Ghetmiri, J. Liu, G. Sun, R. Soref, J. Margetis, J. Tolle, B. Li, Z. Chen, M. Mortazavi, and S. Q. Yu, "Optically Pumped GeSn Lasers Operating at 270 K with Broad Waveguide Structures on Si," ACS Photonics **6**(6), 1434–1441 (2019).
26. J. Chrétien, Q. M. Thai, M. Frauenrath, L. Casiez, A. Chelnokov, V. Reboud, J. M. Hartmann, M. El Kurdi, N. Pauc, and V. Calvo, "Room temperature optically pumped GeSn microdisk lasers," Appl. Phys. Lett. **120**(5), 51107 (2022).
27. A. Bjelajac, M. Gromovyi, E. Sakat, B. Wang, G. Patriarche, N. Pauc, V. Calvo, P. Boucaud, F. Boeuf, A. Chelnokov, V. Reboud, M. Frauenrath, J.-M. Hartmann, and M. El Kurdi, "Up to 300 K lasing with GeSn-On-Insulator microdisk resonators," Opt. Express **30**(3), 3954–3961 (2022).
28. Y. Zhou, Y. Miao, S. Ojo, H. Tran, G. Abernathy, J. M. Grant, S. Amoah, G. Salamo, W. Du, J. Liu, J. Margetis, J. Tolle, Y. Zhang, G. Sun, R. A. Soref, B. Li, and S.-Q. Yu, "Electrically injected GeSn lasers on Si operating up to 100 K," Optica **7**(8), 924–928 (2020).
29. M. Oehme, J. Werner, M. Gollhofer, M. Schmid, M. Kaschel, E. Kasper, and J. Schulze, "Room-Temperature Electroluminescence From GeSn Light-Emitting Pin Diodes on Si," IEEE Photonics Technol. Lett. **23**(23), 1751–1753 (2011).
30. D. Rainko, Z. Ikonic, A. Elbaz, N. von den Driesch, D. Stange, E. Herth, P. Boucaud, M. El Kurdi, D. Grützmacher, and D. Buca, "Impact of tensile strain on low Sn content GeSn lasing," Sci. Rep. **9**, 259 (2019).
31. S. Gupta, B. Magyari-Köpe, Y. Nishi, and K. C. Saraswat, "Achieving direct band gap in germanium through integration of Sn alloying and external strain," J. Appl. Phys. **113**(7), 073707 (2013).
32. A. Elbaz, D. Buca, N. von den Driesch, K. Pantzas, G. Patriarche, N. Zerounian, E. Herth, X. Checoury, S. Sauvage, I. Sagnes, A. Foti, R. Ossikovski, J. M. Hartmann, F. Boeuf, Z. Ikonic, P. Boucaud, D. Grützmacher, and M. El Kurdi, "Ultra-low-threshold continuous-wave and pulsed lasing in tensile-strained GeSn alloys," Nat. Photonics **14**(6), 375–382 (2020).
33. J. Chrétien, N. Pauc, F. Armand Pilon, M. Bertrand, Q. M. Thai, L. Casiez, N. Bernier, H. Dansas, P. Gergaud, E. Delamadeleine, R. Khazaka, H. Sigg, J. Faist, A. Chelnokov, V. Reboud, J. M. Hartmann, and V. Calvo,

"GeSn Lasers Covering a Wide Wavelength Range Thanks to Uniaxial Tensile Strain," ACS Photonics **6**(10), 2462–2469 (2019).
34. R. A. Minamisawa, M. J. Süess, R. Spolenak, J. Faist, C. David, J. Gobrecht, K. K. Bourdelle, and H. Sigg, "Top-down fabricated silicon nanowires under tensile elastic strain up to 4.5%," Nat. Commun. **3**(May), 1096 (2012).
35. S. Wirths, Z. Ikonic, A. T. Tiedemann, B. Holländer, T. Stoica, G. Mussler, U. Breuer, J. M. Hartmann, A. Benedetti, S. Chiussi, D. Grützmacher, S. Mantl, and D. Buca, "Tensely strained GeSn alloys as optical gain media," Appl. Phys. Lett. **103**(19), 192110 (2013).
36. A. Elbaz, R. Arefin, E. Sakat, B. Wang, E. Herth, G. Patriarche, A. Foti, R. Ossikovski, S. Sauvage, X. Checoury, K. Pantzas, I. Sagnes, J. Chrétien, L. Casiez, M. Bertrand, V. Calvo, N. Pauc, A. Chelnokov, P. Boucaud, F. Boeuf, V. Reboud, J. M. Hartmann, and M. El Kurdi, "Reduced Lasing Thresholds in GeSn Microdisk Cavities with Defect Management of the Optically Active Region," ACS Photonics **7**(10), 2713–2722 (2020).
37. F. Gencarelli, B. Vincent, J. Demeulemeester, A. Vantomme, A. Moussa, A. Franquet, A. Kumar, H. Bender, J. Meersschaut, W. Vandervorst, R. Loo, M. Caymax, K. Temst, and M. Heyns, "Crystalline Properties and Strain Relaxation Mechanism of CVD Grown GeSn," ECS J. Solid State Sci. Technol. **2**(4), P134–P137 (2013).
38. S. An, Y. C. Tai, K. C. Lee, S. H. Shin, H. H. Cheng, G. E. Chang, and M. Kim, "Raman scattering study of GeSn under <100> and <110> uniaxial stress," Nanotechnology **32**(35), 355704 (2021).
39. D. Rainko, Z. Ikonic, N. Vukmirović, D. Stange, N. von den Driesch, D. Grützmacher, and D. Buca, "Investigation of carrier confinement in direct bandgap GeSn/SiGeSn 2D and 0D heterostructures," Sci. Rep. **8**(1), 15557 (2018).
40. R. Chen, H. Lin, Y. Huo, C. Hitzman, T. I. Kamins, and J. S. Harris, "Increased photoluminescence of strain-reduced, high-Sn composition Ge1−xSnx alloys grown by molecular beam epitaxy," Appl. Phys. Lett. **99**(18), 181125 (2011).
41. L. Pavesi and M. Guzzi, "Photoluminescence of AlxGa1−xAs alloys," J. Appl. Phys. **75**(10), 4779–4842 (1994).
42. D. Stange, S. Wirths, N. Von Den Driesch, G. Mussler, T. Stoica, Z. Ikonic, J. M. Hartmann, S. Mantl, D. Grützmacher, and D. Buca, "Optical Transitions in Direct-Bandgap Ge1-xSnx Alloys," ACS Photonics **2**(11), 1539–1545 (2015).